Accepted Manuscript

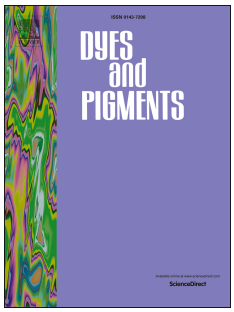

BODIPY derivatives bearing borneol moieties: Enhancing cell membrane permeability for living cell imaging

Jian Yang, Yunshi Fan, Fangjian Cai, Xu Xu, Bo Fu, Shifa Wang, Zhen Shen, Jiangwei Tian, Haijun Xu

PII: S0143-7208(18)32422-7

DOI: https://doi.org/10.1016/j.dyepig.2019.01.012

Reference: DYPI 7285

To appear in: *Dyes and Pigments*

Received Date: 2 November 2018

Revised Date: 31 December 2018

Accepted Date: 9 January 2019

Please cite this article as: Yang J, Fan Y, Cai F, Xu X, Fu B, Wang S, Shen Z, Tian J, Xu H, BODIPY derivatives bearing borneol moieties: Enhancing cell membrane permeability for living cell imaging, *Dyes and Pigments* (2019), doi: https://doi.org/10.1016/j.dyepig.2019.01.012.

BODIPY derivatives bearing borneol moieties: Enhancing cell membrane permeability for living cell imaging

Jian Yang [a,#], Yunshi Fan [b,#], Fangjian Cai [a], Xu Xu [a], Bo Fu [a], Shifa Wang [a], Zhen Shen [c,*], Jiangwei Tian [b,*], Haijun Xu [a,d,*]

[a]*College of Chemical Engineering, Jiangsu Key Lab of Biomass-based Green Fuels and Chemicals, Nanjing Forestry University, Nanjing 210037, P. R. China.*

[b]*State Key Laboratory of Natural Medicines, Jiangsu Key Laboratory of TCM Evaluation and Translational Research, School of Traditional Chinese Pharmacy, China Pharmaceutical University, Nanjing 211198, P. R. China.*

[c]*Nanjing Natl Lab Microstruct, State Key Lab Coordinat Chem, Nanjing University 210046, Jiangsu, P. R. China.*

[d]*Jiangsu Key Laboratory for Biomass Energy and Material, Jiangsu Province, Nanjing 210042, P. R. China.*

 # These authors equally contribute to this work.

*Corresponding author: Dr. and Prof. Haijun Xu

College of Chemical Engineering, Jiangsu Key Lab of Biomass-based Green Fuels and Chemicals, Nanjing Forestry University, Nanjing 210037, P. R. China.

Jiangsu Key Laboratory for Biomass Energy and Material, Jiangsu Province, Nanjing 210042, P. R. China.

Email: xuhaijun@njfu.edu.cn, Phone: +86-25-85427432;

**Corresponding author: Dr. and Prof. Jiangwei Tian

State Key Laboratory of Natural Medicines, Jiangsu Key Laboratory of TCM Evaluation and Translational Research, School of Traditional Chinese Pharmacy, China Pharmaceutical University, Nanjing 211198, P. R. China.

Email: jwtian@cpu.edu.cn，Phone: 86-18260088865

***Corresponding author: Dr. and Prof. Zhen Shen

Nanjing Natl Lab Microstruct, State Key Lab Coordinat Chem, Nanjing University 210046, Jiangsu, P. R. China.

Email: zshen@nju.edu.cn, Phone: 86-25-83621250;

Abstract

Three novel boron-dipyrromethene (BODIPY) dyes bearing borneol moieties have been designed, synthesized and characterized. The single-crystal structure of the compound **3** was also elucidated for the first time. Their photophysical properties and confocal fluorescence images were investigated by the optical spectroscopy and Confocal fluorescence microscopy. The results indicate that the ompounds **2**-**3** take on high fluorescence quantum yield and cell membrane permeability, which can be utilized as fluorescent visualizers for cell and lysosome fluorescence imaging.

Keywords: BODIPY; cell imaging; borneol; photophysical properties; membrane permeability

1. Introduction

Fluorescence imaging has emerged as a very facile and powerful tool to enable the visualization, characterization, and quantification of biological processes that occur at cellular levels without disturbing living subjects in complex biosystems [1-5]. This imaging technique has been widely applied in tumor diagnosis, biomolecule detection, tracking therapeutic effects, the distribution of drug in vivo due to its noninvasion, high spatiotemporal resolution, and real-time visual tracking of biological structures and processes in the living systems [5-8].

Over the past few decades, various of fluorophores with different excitation and emission wavelengths have been designed and developed including coumarin, 1,8-naphthalimide, boron dipyrromethene difluoride (BODIPY), rhodamine, fluoroscein, cyanine, etc [2,9-12]. Among them, the BODIPY derivatives have attracted considerable interest as one of the most promising candidates for fluorescent bio-imaging due to their excellent photophysical properties, such as remarkable fluorescence quantum yields, good biocompatibility, easy modification, sharp fluorescence emission, high photostability, large molar extinction coefficients, and relative insensitivity to environmental conditions [13-15]. In particular, the parent structure of the BODIPY is easily modified, and functional groups can be introduced to the BODIPY core, while retaining their inherent properties. As a result, the BODIPY dyes are widely used for fluorescent bioimaging in medicine and biochemistry [16-18]. However, the big challenge is the poor cell membrane permeability of BODIPY dyes, which limits their application in cell biological imaging [16,19]. So, it is still highly necessary and urgent to design fluorescent BODIPY derivatives with good cell permeability.

It is well known that borneol is a kind of natural chiral compounds. It has many good pharmacological activities and functions, such as analgesic, anti-inflammatory, antibacterial [20]. It can be used as chiral source to synthesize new functional organic compounds. Recently, borneol compounds have been used to improve the cell permeability of drugs which have attracted widespread attention [21]. Borneol can also carry a variety of drugs through the blood-brain barrier and make drugs work better for target organs [22]. To the best of our knowledge, the research has not been published on the synthesis of fluorescent BODIPY derivatives containing borneol moiety and their application in fluorescent imaging yet. In this paper, we have successfully synthesized fluorescent BODIPY derivatives containing borneol group, and report the synthesis, basic photophysical properties and application of these molecules.

2. Results and discussion

2.1. Synthesis

The compounds **1-4** were synthesized according to the routes outlined in Scheme 1. 4-formylbenzoic acid was reacted with excess $SOCl_2$ in the presence of catalytic amount of DMF under reflux to yield 4-formylbenzoyl chloride. Bornyl 4-formylbenzoate was synthesized by treating 4-formylbenzoyl chloride with (-)-Bomeol in the presence of pyridine in THF at room temperature. **1** and **2** were obtained by the reaction of two equivalents of 2, 4-dimethy-pyrrole and 1 equivalent of 4-methoxybenzaldehyde or bornyl 4-formylbenzoate in the presence of a catalytic amount of TFA and subsequently addition of an excess of TEA and $BF_3{\cdot}OEt_2$. **3** and **4** were acquired by the condensation of **2** with bornyl 4-formylbenzoate using the Knoevenagel condensation method [23,24]. All compounds were characterized by elemental analyses, ^{1}H-NMR and HRMS with

satisfactory results. The detailed experimental procedure and characterization data are provided in the ESI.

*2.2. X-ray structure of the compound **3***

The structure of **3** has been determined by X-ray analysis. Fig. 1 shows the perspective view of the molecular conformation of **3**, and there are two crystallographically independent BODIPY molecules in the asymmetric unit. The selected bond lengths and angles are listed in Table S2. The bond lengths for B-N and B-F and the bond angles of N-B-N and F-B-F indicate a tetrahedral BF2N2 geometry and are in good agreement with previously reported data [25,26]. The C20-C21 and C58-C59 bond lengths are both 1.319(5) Å, indicating a double bond character in a trans conformation formed by the condensation reaction between 4,4-difluoro-1, 3, 5, 7-tetramethyl-8-(4-methoxyphenyl)-4-bora-3a,4a-diaza-s-indacene and bornyl 4-formylbenzoate. The bond lengths of C28-O2 and C66-O5 are 1.330(4) Å and 1.317(5) Å, respectively, which is much shorter with respect to the bond distances of C29-O2(1.439(5) Å) and C67-O5 (1.455(5) Å), showing that there are π-electron delocalization within the ester moiety. The meso-C2-C7 phenyl ring and the meso-C40-C45 phenyl ring on the BODIPY core are virtually perpendicular to the corresponding indacene plane with the dihedral angle of 86.38 (0.13) ºand 88.28 (0.13) º, respectively, resulting from the steric hindrance between the 1,7-methyl groups at the 1,7-positions on the indacene moiety and the hydrogen atoms at the 8-position of the meso-phenyl moiety. In addition, the average lengths of the C5-C14 and C43-C52 bond are almost the same length as a single C-C bond, further suggesting almost no π-electron delocalization between the meso-aryl group and the BODIPY core (indacene plane). two indacene planes are highly planar with average root-mean-square (rms) deviation of

0.0101 and 0.0248 Å, respectively. The two dihedral angles of 27.54 (0.17) and 26.92 (0.18) º between the indacene planes and the styryl groups in the two independent BODIPY molecules show partial conjugation within the entire chromophore. There are no π-π stacking interactions between the asymmetrical molecules in compound **3**, which clearly indicates that the introduction of borneol groups can effectively restrain intermolecular π-π stacking.

2.3. Optical properties in solution

The photophysical properties of the compounds **1**-**4** were investigated by absorption as well as steady-state and time-resolved fluorescence spectroscopy in toluene. The photophysical data are summarized in Table 1. The normalized absorption and fluorescence spectra of the compounds **1**-**4** are depicted in Fig. 2. The compounds **1** and **2** share the common BODIPY framework, and the only difference is the substituents of the meso position. Therefore, they exhibit similar absorption and emission spectra. As shown in Fig. 2, the absorption maxima of the compounds **1** and **2** are centred at approximately 518 nm and 514 nm with molar absorption coefficients in the range 23000-72000 $M^{-1}cm^{-1}$, respectively, which can be ascribed to the strong $S_0 \rightarrow S_1$ transitions. For the compound **3** and **4**, with one or two phenyl styryl groups extending the π-conjugation, their absorption maxima were found to redshift to 568 nm and 640 nm, respectively. At higher energies, the compounds **3** and **4** also show strong absorption at 333 nm and 362 nm, which are are attributed to S_0-Sn ($n \geq 2$) transitions [27]. In addition, the weaker and broader shoulders appearing at around 528 nm and 589 nm for **3** and **4** were observed at low wavelength, which are attributed to the 0–1 vibrational transition of the BODIPY moiety [28,29]. As shown in Fig. 2, the emission

bands of the compounds **1**-**4** are good mirror images of their $S_0 \rightarrow S_1$ transition bands with a small Stokes shift between 240 and 458 cm^{-1}, similar to classical meso-aryl BODIPYs and centred at 518 nm, 514 nm, 577 nm and 650 nm, respectively. The fluorescence quantum yields of compounds **1**-**3** determined in non-polar toluene were were higher than that of compound **4**. Thus compounds **1**-**3** were beneficial to biological fluorescence imaging research. The fluorescence quantum yields of **1** and **2** are 0.39 and 0.37, respectively, and they are almost equal. It was noteworthy that the fluorescence quantum yield of **3** is 0.41, which are higher than that of **2**. Such an improvement is different from the ordinary mono- or di-styryl-substituted BODIPY analogues and mainly attributed to the rigid steric effects of borneol moieties which limited the nonradioactive relaxation, thus the fluorescence quantum yield is increased. However, **4** exhibits much weaker fluorescence compared with **2** and **3**. 4-methoxylphenyl group is typical electron-donating group, whereas ester group was a strong electron-withdrawing group. In the excited state, strong intramolecular charge transfer would happen between meso-4-methoxylphenyl group and two ester groups, which led to low quantum yields [30]. In addition, fluorescence lifetimes of **1**-**3** were also measured with τ values in the range of 2.6 to 4.86 ns. These photophysical properties account for a very rigid system exhibiting a very little loss of energy via non radiative pathway [31,32]. This last point is confirmed by low non radiative kinetic constants compared with the radiative ones (Table 1). The rate constant of radiative (k_r) and nonradiative (k_{nr}) deactivation can be calculated from the measured Φ_f and the single-exponential fluorescence lifetime τ according to equations in the literature [33]. Non-radiative (k_{nr}) rate constants are far more dependent on the Bodipy structure [34]. According to Table 1, the very rigid system in compound **2** makes the compound reducing loss of energy via non radiative pathway

compared to compound **1**, the same with conpounds **3** and **4**.

*2.4. Cell-imaging of the compounds **1-4***

HeLa cells are human cervical carcinoma cells with strong proliferative capacity and easy to culture for cell imaging research[35,36]. Therefore, HeLa cell line is chosen as the model to investigate the intracellular localization of BODIPY derivatives by confocal fluorescence imaging. HeLa cells were incubated with BODIPY compounds bearing borneol and performed with confocal fluorescence imaging (Fig.3-4). Compound **1** as a control incubated with HeLa cells showed that the fluorescence of BODIPY was in cytoplasm (Fig. 3). After incubated with 2.0 μM compound **3** for 1 h, the fluorescence almost filled the entire cell and distributed throughout the cytoplasm and nucleus, indicating excellent membrane penetrability of compound **3**. In contrast, the intracellular fluorescence appeared very weak after incubated with 2.0 μM compound **4** under the same condition, which could be attributed to the low fluorescence quantum yield of compound **4**. Notably, cells stained with compound **2** showed remarkable fluorescence in discrete subcellular locations. To further determine the distribution site of compound **2**, co-staining experiments with LysoTracker Green and Hoechst 33342 has been carried out. As seen from the overlay images, the fluorescence ascribable to compound **2** co-localized well with LysoTracker Green (Fig. 4). The result was further confirmed by stack image for Z-depth scanning of Compound **2**-loaded cells, suggesting that Compound **2** has high lysosome-targeting capability. The different cellular localization of compounds **2** and **3** in HeLa cells may be due to the different substitutional positions of borneol group.

3. Conclusion

In summary, we have designed and synthesized three new BODIPY derivatives (Compounds **2**-**4**) containing borneol moieties which show excellent fluorescence properties. Confocal fluorescence microscopy experiments have indicated the compounds **2** and **3** possess good cell membrane permeability. In particular, **2** has high lysosome-targeting capability, which is highly promising for practical applications such as tumor diagnosis.

4. Experimental section

4.1. General

All chemicals and solvents were of commercial quality and used without further purification unless otherwise indicated. Dry CH_2Cl_2 was distilled from CaH_2 under nitrogen. The reactions to synthesize the compounds **1** and **2** were carried out under an N_2 atmosphere. Analytical thin-layer chromatography was performed on Kieselgel 60 F254 (Merck). The photo-physical properties was mesured by LAMBDA 950 UV/Vis Spectrophotometer, PerkinElmer LS 55 Fluorescence spectrometer and a FluoroLog-UltraFast (HORIBA Instrument Inc, Edison) spectrometer. ^{1}H NMR spectra were recorded on a Bruker DRX-600 AVANCE III spectrometer. Chemical shifts for ^{1}H NMR spectra were expressed in parts per million (ppm) relative to $CDCl_3$ (δ = 7.26 ppm) as the internal standard. The High Resolution Mass Spectra (HRMS) data were obtained on a LTQ Orbitrap XL spectrometer in ESI mode. All the solvents employed for the spectroscopic measurements were of spectroscopic grade (Aldrich).

Cell culture. Human cervical carcinoma HeLa cell lines were obtained from KeyGEN Biotech (Nanjing, China). Both cell lines were cultured in Dulbecco's modified Eagle's medium (DMEM) containing 10% fetal bovine serum (FBS), 100 $\mu g \cdot mL^{-1}$ streptomycin

and 100 $U \cdot mL^{-1}$ penicillin at 37 °C in a humidified incubator containing 5% CO_2 and 95% air. The medium was replenished every other day and the cells were subcultured after reaching confluence. Cell numbers were determined with a Petroff-Hausser cell counter (USA).

HeLa cells were seeded into 35-mm confocal dishes (Glass Bottom Dish) at a density of 1×10^4 per dish and incubated for 24 h at 37 °C. The medium was then replaced with fresh serum-free culture medium containing 2.0 μM compound and incubated at 37 °C for 1 h. Before imaging, the cells were washed with PBS and further incubated with 1.0 μM LysoTracker® Green and 1.0 μM Hoechst 33342 for 15 min. The fluorescence of cells was visualized with a confocal laser scan microscopy at stationary parameters including the laser intensity, exposure time and objective lens. Compound **1** and **2** was excited with a 488 nm laser and emission was collected from 550 to 600 nm. Compound **3** was excited with a 532 nm laser and emission was collected from 550 to 600 nm. Compound 4 was excited with a 532 nm laser and emission was collected from 600 to 650 nm.

X-ray structure determination. X-ray single-crystal diffraction data were collected on a Bruker smart II diffractometer with Mo–Kα radiation (λ = 0.71073 Å). Data collection and procees was completed by using the Bruker Smart and Saint (Bruker). Empirical absorption corrections were performed with SADADS. The structures were solved by direct methods and refined by the full-matrix method based on F^2 by means of the SHELXLTL software package. Non-H atoms were refined anisotropically using all reflections with $I > 2\sigma(I)$. All H atoms were generated geometrically and refined using a "riding" model with Uiso = 1.2Ueq (C and N). The CCDC deposition No. 1859519 for **3** containing the supplementary crystallographic data for this paper. These data can be

obtained free of charge via www.ccdc.cam.ac.uk/conts/retrieving.html (or from the Cambridge Crystallographic Data Centre, 12 Union Road, Cambridge CB21EZ, UK; fax: (+44)1223–336–033; E-mail: deposit@ccdc.cam.ac.uk).

Spectroscopic measurements. UV-visible absorption spectra were carried out on a Shimadzu UV-3100 spectrophotometer. Fluorescence spectra were measured PerkinElmer LS 55 Fluorescence spectrometer. The fluorescence life time of the samples were determined with a FluoroLog-UltraFast (HORIBA Instrument Inc, Edison) spectrometer equipped with a 450 W CW xenon lamp and an Open-Electrode TECooled CCD Detector (Syncerity). Nanosecond lifetime and TRES studies were conducted using a TCSPC MCA model equipped with a picosecond photodetector (<200 ps) (PPD850) and picosecond laser (duration is 180 ps, Deltadiode, 100 MHz laser). TRES data were measured by incrementing the monochromator on the emission channel of the time-resolved fluorometer in fixed wavelength intervals at each wavelength. Slices of data were taken in the intensity-wavelength plane to obtain spectra at different times during the decay. Microsecond lifetime decays were collected by a MCS mode on TCSPC HUB（DeltaHUB）with a LED source (SpectraLED) as a sample excitation source. DeltaDiode-405 and -635 were used for lifetime measurements. Absorption and emission measurements were carried out in 1×1 cm quartz cuvettes. For all measurements, the temperature was kept constant at 298 K. Dilute solutions with absorbance of less than 0.05 at the excitation wavelength were used for the measurement of fluorescence quantum yields. Rhodamine B was used as the standard (Φ_F = 0.5 in ethanol) [37]. The quantum yield, Φ, was calculated using equation (1):

$$\Phi_{sample}=\Phi_{std}\times(I_{sample}/I_{std})\times (A_{std}/A_{sample}) \times (n_{sample}/n_{std}) \qquad (1)$$

Where the sample and std subscripts denote the sample and standard, respectiveluy. *l* is the integrated emission intensity. *A* stands for the absorbance, and *n* is the refractive index.

When the fluorescence decays were monoexponential, the rate constants of radiative (k_r) and nonradiative (k_{nr})deactivation were calculated from the measured fluorescence quantum yield (Φ_F) and fluorescence lifetime (τ) according to equations (2) and (3):

$$k_r = \Phi_F/\tau \quad (2)$$

$$k_{nr} = (1-\Phi_F)/\tau \quad (3)$$

*4.2. Synthesis of Compounds **1-4***

*4.2.1. Compound **1***. Compound **1** was synthesized according to procedures described previously [38].

*4.2.2 The synthesis of **Bornyl 4-formylbenzoate**. Terephthalaldehydic acid 1.58 g (10 mmol), thionyl chloride 10 mL and N,N-dimethylformamide in a catalytic amount* were added to a 100 ml eggplant-shaped flask equipped with a condenser and calcium chloride tube. The reaction mixture was refluxed for 10 hours. After cooling to room temperature, and the solvents were removed in vacuo, and the crude product was used immediately without further purification.

A solution of (-)-Bomeol 1.62 g (10 mmol) and pyridine in a catalytic amount in 15 mL dry CH_2Cl_2 was cooled to 0 °C in an ice bath while stirring under a nitrogen atmosphere. To this solution 4-formylbenzoyl chloride in CH_2Cl_2 (10 mL) was added dropwise under ice-bath during 1 hour, and the reaction was left to stir for further 12 hours at room temperature. After the reaction was completed, water was added and the mixture was extracted three times with CH_2Cl_2. The combined organic phases were washed with saturated $NaHCO_3$ solution, and dried over Na_2SO_4. After filtration and the solvent was removed in vaccuo to obtain a pale yellow oil. The product was purified by column chromatography[SiO_2, CH_2Cl_2-hexane (1:1)] to yield the white solid product 1.71g (Yield: 60%) ^{1}H NMR (600 MHz, $CDCl_3$) δ 10.11(s, 1 H), 8.21(d, $^3J_{HH}$ = 8.4 Hz,

2 H), 7.96(d, $^3J_{HH}$ = 7.8 Hz, 2 H), 5.16- 5.13(m, 1 H), 2.53- 2.47(m, 1 H), 2.14- 2.09(m, 1 H), 1.86- 1.80(m, 1 H), 1.76(t, $^3J_{HH}$ = 4.8 Hz, 1 H), 1.47- 1.41(m, 1 H), 1.35- 1.30(m, 1 H), 1.13(dd, $^3J_{HH}$ = 3.0, 13.8 Hz, 1 H), 0.98(s, 3 H), 0.93(s, 6 H).

*4.2.3. Compound **2**.* A 250 mL three necked flask was used for the reaction. Bornyl 4-formylbenzoate (2 mmol, 0.5727 mg) was dissolved in dry dichloromethane. After the solvent was bubbled by N_2 for 20 min, 2,4-dimethyl-1H-pyrrole (4 mmol, 412 µL) was added. Then trifluoroacetic acid (50 µL) was added drop by drop with a syringe while covered from light. After the reaction continued for 5 h, DDQ (2 mmol, 0.454 g) was added and the solvent was stirred for 1 h. After that, Et_3N and BF_3•OEt_2 were followed and stirred for 2 h. The solvent was washed by water and Organic phase dried over Na_2SO_4, evaporated and residue was purified by silica gel column chromatography using DCM: PE (3 : 7) as the eluent, yielded the desired compound **2** as orange powder (139.4 mg, 13.8%).^{1}H NMR (600 MHz, $CDCl_3$): δ 8.18 (d, $^3J_{HH}$ = 8.4 Hz, 2H), 7.41 (d, $^3J_{HH}$ = 8.4 Hz, 2 H), 6.00 (s, 2 H), 5.17-5.14 (m, 1 H), 2.56 (s, 6 H), 2.54-2.49 (m, 1 H), 2.18-2.13 (m, 1 H), 1.87-1.81 (m, 1 H), 1.78 (t, $^3J_{HH}$ = 16.2 Hz, 1 H), 1.56-1.55 (m, 1 H), 1.38 (s, 6 H), 1.36-1.33 (m, 1 H), 1.19-1.16 (m, 1 H), 0.99 (s, 3 H), 0.95 (d, $^4J_{HH}$ = 9.6 Hz, 6 H). λ_{max} (ε)(in Toluene) = 514 nm (72420 L·mol^{-1}·cm^{-1}). m/z (HRMS): calcd [M^+] for $C_{30}H_{35}BF_2N_2O_2$: 504.2760, found: 504.2820.

*4.2.4. Compounds **3** and **4**.* Compound **1** (0.2 mmol, 70.8 mg) and borneol aldehyde (0.4 mmol, 114.4 mg) were added to a 50 mL round bottomed flask containing 25 mL toluene and to this solution was added piperidine (2 mL) and PTSA (35 mg). The mixture was heated under reflux by using a Dean-Stark trap and reaction was monitored by TLC DCM : PE (1 : 1). When the starting material compound **1** had been consumed, the mixture was cooled to room temperature and solvent was evaporated. Water (100 mL) added to the residue and the product was extracted into the CH_2Cl_2 (3×100 mL). Organic phase dried over Na_2SO_4, evaporated and residue was purified by silica gel column chromatography using DCM: PE (1 : 1) as the eluent, yielded the desired compound **3** as black powder (10 mg, 8%) and compound **4** (23 mg, 12.9 %). Compound **3** ^{1}H NMR (600 MHz, $CDCl_3$): δ 8.04 (d, $^3J_{HH}$ = 8.4 Hz, 2 H), 7.77 (d, $^3J_{HH}$ = 16.8 Hz, 1 H), 7.64 (d, $^3J_{HH}$ = 7.8 Hz, 2 H), 7.23-7.20 (m, 3 H), 7.03 (d, $^3J_{HH}$ = 9.0 Hz, 2 H), 6.62 (s, 1 H), 6.04 (s, 1 H), 5.14-5.11 (m, 1 H), 3.89 (s, 3 H), 2.61 (s, 3 H), 2.51-2.46 (m, 1 H), 2.17-2.12 (m, 1 H), 1.85-1.79 (m, 1 H), 1.75 (t, $^3J_{HH}$ = 9.0 Hz, 1 H),

1.49 (s, 3 H), 1.47 (s, 3 H), 1.35-1.30 (m, 2 H), 1.16-1.13 (m, 1 H), 0.98 (s, 3 H), 0.93 (s, 6 H). λ_{max} (ε)(in Toluene) = 568 nm (72330 $L \cdot mol^{-1} \cdot cm^{-1}$). m/z (HRMS): calcd [$M^+$] for $C_{38}H_{41}BF_2N_2O_3$: 622.3178, found: 622.3176. Compound **4** ^1H NMR (600 MHz, $CDCl_3$): δ 8.09 (d, $^3J_{HH}$ = 8.4 Hz, 4 H), 7.84 (d, $^3J_{HH}$ = 16.2 Hz, 2 H), 7.70 (d, $^3J_{HH}$ = 7.8 Hz, 4 H), 7.29 (s, 2 H), 7.23 (d, $^3J_{HH}$ = 8.4 Hz, 2 H), 7.05 (d, $^3J_{HH}$ = 8.4 Hz, 2 H), 6.68 (s, 2 H), 5.15-5.13 (m, 2 H), 3.90 (s, 3 H), 2.52-2.47 (m, 2 H), 2.19-2.14 (m, 2 H), 1.86-1.80 (m, 2 H), 1.76 (t, $^3J_{HH}$ = 9.0 Hz, 2 H), 1.52 (s, 6 H), 1.37-1.26 (m, 4 H), 1.17-1.14 (m, 2 H), 0.99 (s, 6 H), 0.94 (s, 12 H). λ_{max} (ε)(in Toluene) = 640 nm (79930 $L \cdot mol^{-1} \cdot cm^{-1}$). m/z (HRMS): calcd [$M^+$] for $C_{56}H_{61}BF_2N_2O_5$: 890.4642, found: 890.4690.

Acknowledgements

Financially supported by National Key R&D Program of China (2016YFD0600804), National Natural Scientific Foundation of China (No. 21301092, 21606133), Natural Scientific Foundation of Jiangsu Province, P. R. China (No. BK20151513), the Fok Ying Tung Education Foundation (Grant No. 141030), and the open Fund of Jiangsu Key Laboratory for Biomass Energy and Material(JSBEM201702).

Appendix A. Supplementary data

Supplementary data related to this article can be found at http:// xxxxxxxxxxxx.

References

[1] Zheng Q, Xu G, Prasad P N. Conformationally restricted dipyrromethene boron difluoride (BODIPY) dyes: highly fluorescent, multicolored probes for cellular imaging. Chem-Eur J 2010; 14: 5812-5819.

[2] Zhang M, Zheng S T, Liu X J, et al. A series of novel NIR fluorescent dyes: Synthesis, theoretical calculations and fluorescence imaging applications in living cells. Dyes Pigments 2016; 125: 220-228.

[3] Cho D G, Sessler J L. Modern Reaction‐Based Indicator Systems. Chem Soc Rev 2009; 38: 1647-1662.

[4] Qian X, Xiao Y, Xu Y, et al. "Alive" Dyes as Fluorescent Sensors: Fluorophore, Mechanism, Receptor and Images in Living Cells. Chem Commun 2010; 46: 6418-6436.

[5] Liu B, Luo Z, Si S, et al. A photostable triphenylamine-based flavonoid dye: Solvatochromism, aggregation-induced emission enhancement, fabrication of organic nanodots, and cell imaging applications. Dyes Pigments 2017; 142: 32-38.

[6] Chan J, Dodani S C, Chang C J. Reaction-based small-molecule fluorescent probes for chemoselective bioimaging. Nat Chem 2012; 4: 973-984.

[7] Hong G, Lee J C, Robinson J T, et al. Multifunctional in vivo vascular imaging using near-infrared II fluorescence. Nat Med 2012; 18: 1841-1846.

[8] Alford R, Ogawa M, Hassan M, et al. Fluorescence lifetime imaging of activatable target specific molecular probes. Contrast Media Mol Imaging 2010; 5: 1-8.

[9] Ashton T D, Jolliffe K A, Pfeffer F M. Luminescent probes for the bioimaging of small anionic species in vitro and in vivo. Chem Soc Rev 2015; 44: 4547-4595.

[10] Lee M H, Kim J S, Sessler J L. Small molecule-based ratiometric fluorescence probes for cations, anions, and biomolecules. Chem Soc Rev 2015; 44: 4185-4191.

[11] Zhao Y, Ren Y, Li H, et al. A new far-red naphthorhodamine dye: Synthesis, fluorescent probe and bioimaging applications. Dyes Pigments 2016; 132: 255-261.

[12] Gao Z, Zhang X, Chen Y. One-pot synthesis of a near-infrared fluorophore for living cells imaging. Dyes Pigments 2017; 140: 56-61.

[13] Zhu S, Dorh N, Zhang J, et al. Highly water-soluble neutral near-infrared emissive BODIPY polymeric dyes. J Mater Chem 2012; 22: 2781-2790.

[14] Wang B, Li P, Yu F, et al. A near-infrared reversible and ratiometric fluorescent probe based on Se-BODIPY for the redox cycle mediated by hypobromous acid and hydrogen sulfide in living cells. Chem Commun 2013; 49: 5790-5792.

[15] Lu H, Mack J, Yang Y, et al. Structural modification strategies for the rational design of red/NIR region BODIPYs. Chem Soc Rev 2014; 43: 4778-4823.

[16] Kowada T, Maeda H, Kikuchi K. ChemInform Abstract: BODIPY-Based Probes for the Fluorescence Imaging of Biomolecules in Living Cells. Chem. Soc. Rev. 2015; 44: 4953-4972.

[17] Wang S S, Liu H, Mack J, et al. A BODIPY-based 'turn-on' fluorescent probe for hypoxic cell imaging. Chem Commun 2015; 51: 13389-13392.

[18] Lu H, Xiong L, Liu H, et al. A highly selective and sensitive fluorescent turn-on sensor for Hg^{2+} and its application in live cell imaging. Org Biomol Chem 2009; 7: 2554-2558.

[19] Wang K P, Xiao Y J, Wang Y Y, et al. Self-assembled hydrophobin for producing water-soluble and membrane permeable fluorescent dye. Sci Rep 2016; 6: 23061-23071.

[20] Dai J, Chen J, Bei Y, et al. Influence of borneol on primary mice oral fibroblasts: a penetration enhancer may be used in oral submucous fibrosis. J Oral Pathol Med 2010; 38: 276-281.

[21] Zhang Q L, Fu B M, Zhang Z J. Borneol, a novel agent that improves central nervous system drug delivery by enhancing blood-brain barrier permeability. Drug Delivery 2017; 24: 1037-1044.

[22] Yu B, Ruan M, Dong X, et al. The mechanism of the opening of the blood-brain barrier by borneol: A pharmacodynamics and pharmacokinetics combination study. J Ethnopharmacol 2013; 150: 1096-1108.

[23] Mani V, Krishnakumar V G, Gupta S, et al. Synthesis and characterization of styryl-BODIPY derivatives for monitoring in vitro Tau aggregation. Sens Actuators B 2017; 244: 673-683.

[24] Wang C, Xia X, Luo J, et al. A novel near-infrared styryl-BODIPY fluorescent probe for discrimination of GSH and its application in living cells. Dyes Pigments 2018; 152: 85-92.

[25] Yin Z, Tam A Y, Wong K M, et al. Functionalized BODIPY with various sensory units--a versatile colorimetric and luminescent probe for pH and ions. Dalton Trans 2012; 41: 11340-11350.

[26] Shen Z, Röhr H, Rurack K, et al. Boron-diindomethene (BDI) dyes and their tetrahydrobicyclo precursors--en route to a new class of highly emissive fluorophores for the red spectral range. Chem-Eur J 2010; 10: 4853-4871.

[27] Bura T., Retailleau P., Ulrich G., et al. Highly Substituted Bodipy Dyes with Spectroscopic Features Sensitive to the Environment J Org Chem 2011; 76, 1109–1117.

[28] Uppal T, Hu X, Fronczek F R, et al. Synthesis, Computational Modeling, and Properties of Benzo-Appended BODIPYs. Chem-Eur J 2012; 18: 3893-3905.

[29] Galangau O, Dumasverdes C, Méalletrenault R, et al. Rational design of visible and NIR distyryl-BODIPY dyes from a novel fluorinated platform. Org Biomol Chem 2010; 8: 4546-4553.

[30] Xu J, Zhu L, Wang Q, et al. meso-C6F5, substituted BODIPYs with distinctive spectroscopic properties and their application for bioimaging in living cells. Tetrahedron 2014; 70: 5800-5805.

[31] Guerin C, Gerard L J, Octobre G, et al. Bis-triazolyl BODIPYs: a simple dye with strong red-light emission. RSC Adv. 2015; 5: 76342-76345.

[32] Umezawa K, Nakamura Y, Makino H, et al. Bright, Color-Tunable Fluorescent Dyes in the Visible-Near-Infrared Region. J Am Chem Soc 2008; 130: 1550-1551.

[33] Qin W, Baruah M, Stefan A, et al. Photophysical Properties of BODIPY-Derived Hydroxyaryl Fluorescent pH Probes in Solution. ChemPhysChem 2005; 6: 2343-2351.

[34] Benniston A. C. and Copley G. Lighting the way ahead with boron dipyrromethene (Bodipy) dyes. Phys Chem Chem Phys 2009; 11: 4124-4131.

[35] Li D., Xu Y., Zhou N., Liu J., Wang R., Cheng T., Tang Y., Zhu W., Xu Y., Qian X. A novel ‘‘donor-two-acceptor’’ type fluorophore-based probe for fast detection and intracellular imaging of nitroreductase Dyes Pigment. 2017; 136: 627-632.

[36] Li Z., Li X., Gao X., Zhang Y., Shi W., Ma H. Nitroreductase Detection and Hypoxic Tumor Cell Imaging by a Designed Sensitive and Selective Fluorescent Probe, 7-[(5- Nitrofuran-2-yl)methoxy]-3H-phenoxazin-3-one Anal. Chem., 2013, 85, 3926-3932.

[37] Albert M. Brouwer. Standards for photoluminescence quantum yield measurements in solution. Pure. Appl. Chem. 2011; 83: 2213–2228.

[38] Qiao L, Nie H, Wu Y, et al. An ultrafast responsive BODIPY-based fluorescent probe for the detection of endogenous hypochlorite in live cells. J Mater Chem B 2016; 5: 525-530.

Figure Captions

Scheme 1. Structures and synthesis of Compounds **1**-**4**.

Fig. 1. Perspective views of **3**, showing 30% probability displacement ellipsoids (hydrogen atoms and ethyl ether molecule are deleted for clarity).

Fig. 2. Normalized UV/Vis (a) and fluorescence (b) spectra of BODIPYs **1** (blue), **2** (green), **3** (black) and **4** (red) in toluene at 25 ℃.

Fig. 3. Confocal fluorescence images and bright-field images of HeLa cells incubated with 2.0 μM compounds at 37 °C for 1 h.

Fig. 4. Confocal fluorescence images, bright-field images and three-dimensional fluorescence images of compound **2**-loaded HeLa cells stained with LysoTracker green and Hoechst 33342 for 1 h at 37 °C.

Table 1. Photophysical properties of the compounds **1**-**4** in toluene. [a] the compounds **1** and **2** were excited at 488 nm, the compounds **3** and **4** were excited at 520 nm, 570 nm respectively.

Scheme 1.

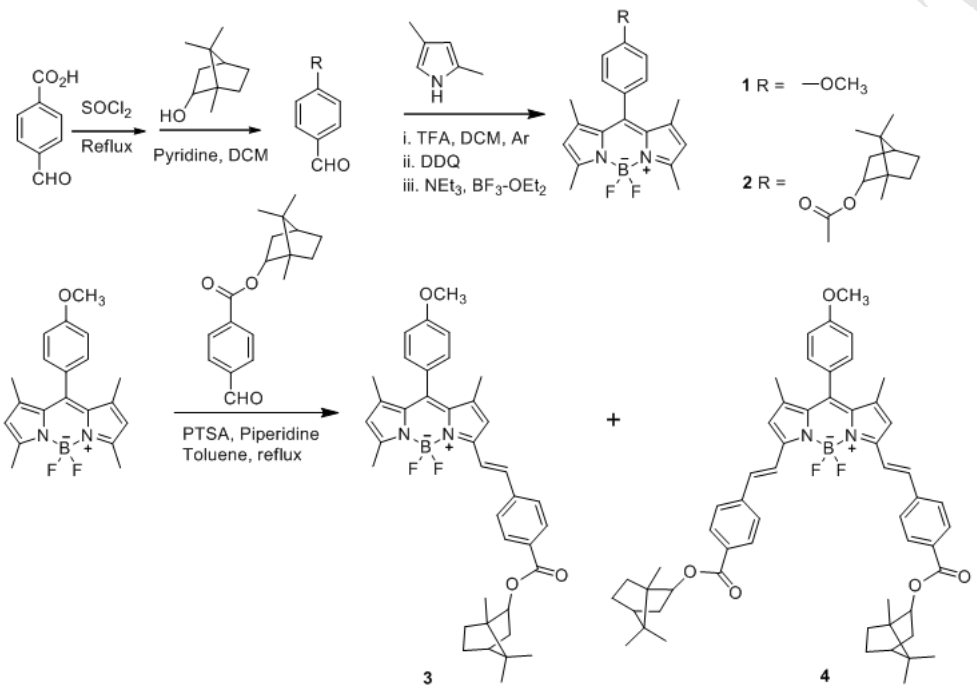

Fig. 1.

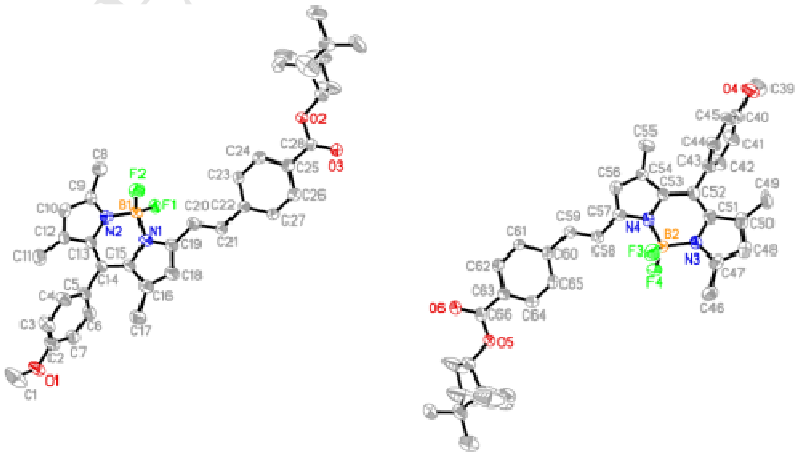

Fig. 2.

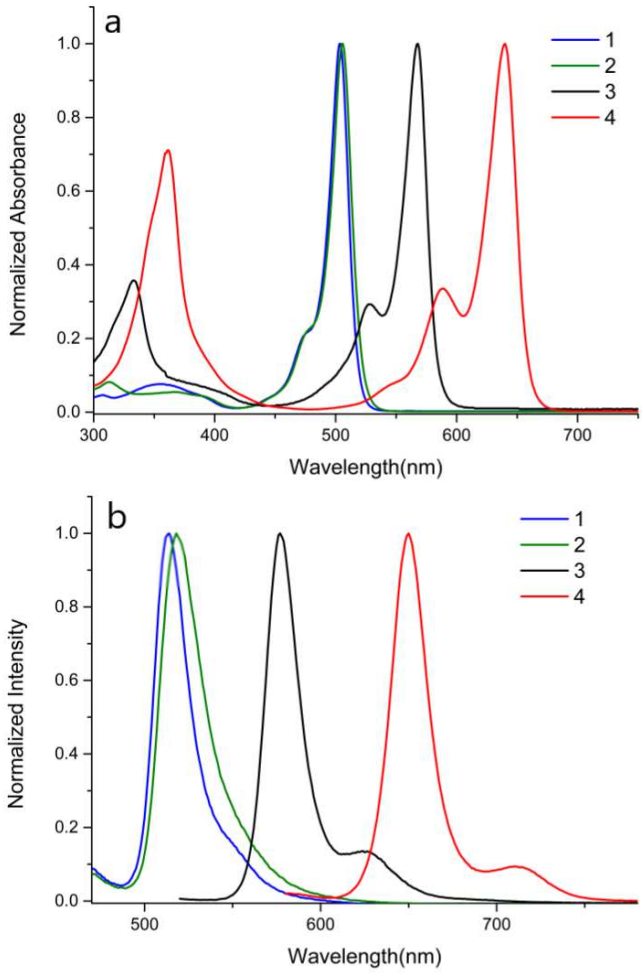

Fig. 3.

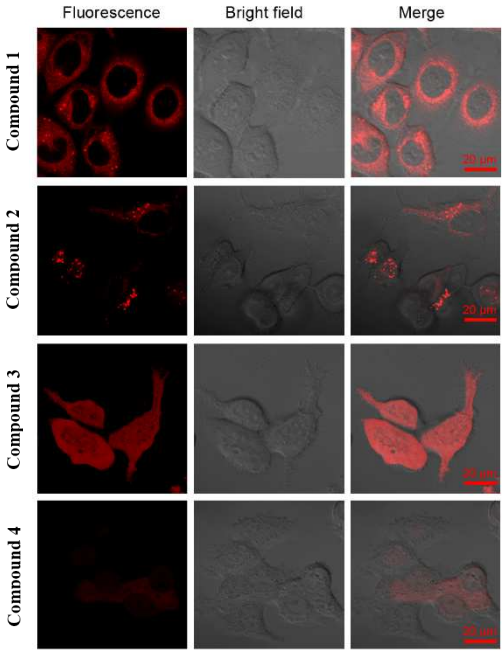
Fluorescence
Bright field
Merge
Compound 1
Compound 2
Compound 3
Compound 4

Fig. 4.

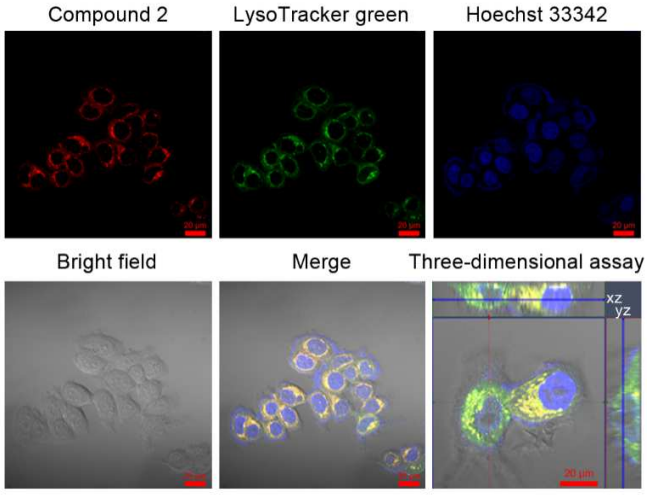
Compound 2
LysoTracker green
Hoechst 33342
Bright field
Merge
Three-dimensional assay
xz
yz

Table 1

	λ_{abs} [nm]	λ_{em}[a] [nm]	$\Delta\upsilon$ [cm^{-1}]	Φ_F	τ_F [ns]	κ_r [10^8 s^{-1}]	κ_{nr} [10^8 s^{-1}]
1	504	514	386	0.39	4.86	0.84	1.21
2	506	518	458	0.37	2.30	1.61	2.74
3	568	627	275	0.41	3.82	1.15	1.47
4	640	710	240	0.061	2.60	0.16	3.72

Highlights:

1. Three novel boron-dipyrromethene (BODIPY) dyes bearing borneol moieties have been synthesized and take on excellent cell membrane permeability.

2. The compounds **2**-**3** show high fluorescence quantum yield, and can be utilized as fluorescent visualizers for cell and lysosome fluorescence imaging.